DOI: https://doi.org/10.54966/jreen.v1i3.1290

Journal of Renewable Energies

Revue des Energies Renouvelables

journal home page: https://revue.cder.dz/index.php/rer

Conference paper

Experimental Investigation of a Vertical Axis Savonius Wind Turbine

Kawther Berrahi [a,*], **Hidayet Meroua Sefiani** [b], **Abdelkader Benaziza** [a,b], **Mohammed El Amine Feraoun** [a,b]

[a] *Faculty of Mechanical Engineering, USTO-MB University, Oran 31000, Algeria*

ARTICLE INFO

Article history:

Received September 30, 2024

Accepted October 22, 2024

Keywords:

Vertical axis wind turbine (VAWT),
Horizontal axis wind turbine (HAWT),
Savonius rotor,
Wind tunnel,
Generator,
Blade,
Buckets.

ABSTRACT

Wind turbines are machines that convert wind energy into energy usable by humans. These include wind turbines that produce electricity or those that pump water. There are many models of wind turbines.This report proposes to study an experimental part of a Savonius vertical axis wind turbine. We then define the efficiency of our Savonius wind turbine by its energy (the electrical output power over the kinetic power of the input wind). The parameters studied are varied: geometric configuration of the rotor, influence of the speed of the wind, influence of the generator, The study was carried out using a blower (reverse mode of a vacuum cleaner), The one of the shortcomings of the Savonius model is its relatively low efficiency, it is interesting to know which energy transformations (transformation of wind energy into mechanical energy of rotation, and transformation of mechanical energy of rotation into electrical energy) lead to yields so weak.

1. INTRODUCTION

Wind power, derived from the force of the wind, has become a major source of renewable energy worldwide. Among the many wind turbine technologies, the Savonius type rotor occupies an important place due to its vertical-axis design and its ability to operate efficiently in variable wind conditions, while drawing on the contributions of several researchers who have explored various aspects of Savonius rotors through wind tunnel experiments and in-depth analysis. Firstly, research by Saha et al. (2008) assessed the aerodynamic performance of single-, two- and three-stage Savonius rotors. Their tests covered a range of parameters, including blade aspect ratio, blade overlap and spacing, and the addition of tip extensions and tip plates. Their results showed the importance of these factors in maximizing rotor

* *Corresponding author, E-mail address: kawther.berrahi@univ-usto.dz*
Tel : + 213 558197626

ISSN: 1112-2242 / EISSN: 2716-8247

energy efficiency Similarly, Mojola (1985) analyzed the performance of Savonius rotors under real-life conditions, focusing on wind speed, torque and power output. His research led to the definition of design standards for these rotors, providing guidelines for their optimization. Meanwhile, Ricci et al. (2016) have studied the performance of a Savonius rotor for use in an innovative streetlight, examining the impact of different construction methods on its performance. Their work identified optimal configurations, including the addition of end plates, to improve the rotor's efficiency under real-life conditions. Finally, experiments by Alexander et al. (1978) tested various Savonius rotor configurations in a wind tunnel. Their results highlighted the significant effect of blade aspect ratio on rotor efficiency, as well as the importance of certain additions, such as tip plates, in maximizing performance. In this study, we build on this previous research to deepen our understanding of Savonius rotors and propose recommendations for their optimal design and use.

2. PRESENTATION OF THE UNIVERSITY WIND TUNNEL

The TE 44 Subsonic Wind Tunnel, located at the Faculty of Mechanical Engineering, is an essential facility for aerodynamic research. This subsonic wind tunnel features a horizontal closed-loop configuration, offering compactness and convenience for exploring aerodynamic phenomena. Designed according to conventional standards, it distinguishes itself with numerous advantages compared to similar open-loop wind tunnels. Among these advantages are a high maximum velocity of 60 m/s, optimized energy efficiency, and low noise levels, making this equipment a valuable tool for studies in the field of aerodynamics detailed view as shown in Fig. 1.

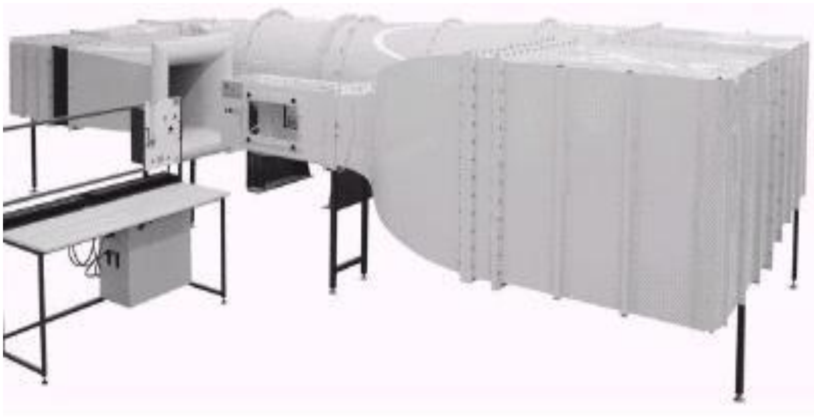

Fig 1. TE44 subsonic wind tunnel

3. THE STEPS OF THIS EXPERIMENTAL STUDY

In this study, a crucial aspect was the access to the assembly and disassembly of the wind turbine model as well as the wind tunnel balance. This manipulation not only enables efficient installation and removal of the wind turbine model for testing purposes but also allows adjustment of the wind tunnel balance to ensure precise and reproducible experimental conditions. The ability to perform these operations efficiently and accurately is essential to ensure the validity and reliability of the results obtained during wind tunnel tests. Figures 2 and 3 illustrate that these aspects are crucial for the successful conduct of experiments.

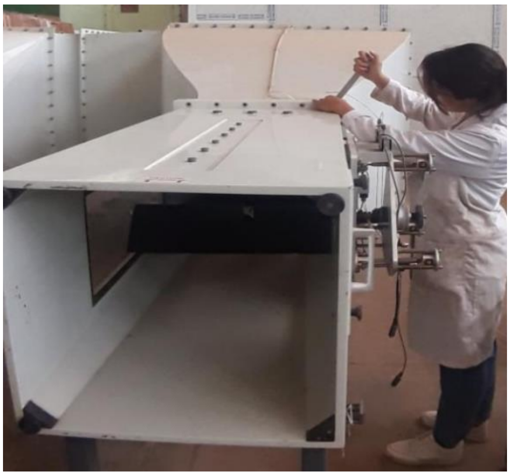

Fig 2. Removing the turbine on the side

Fig 3. Mounting the wind of the wind tunnel blower scale

In this context, Fig. 4 shows that during the assembly of the wind turbine, we encountered a technical challenge. The diameter of the pulley was smaller than that of the wind turbine mast, requiring an adjustment to ensure proper assembly. To address this issue, we had to bore the central part of the pulley, removing a thickness of 0.7 mm. This delicate operation was necessary to ensure a safe and functional assembly of the wind turbine, underscoring the importance of precision in mechanical adjustments during prototype construction. Once this operation is completed, as shown in Fig. 5, the wind turbine mast is securely attached to the central part of the pulley using the welding process. This step is essential to ensure the stability of the assembly and enable effective consolidation of our materials.

Fig 4. Lathe machining of pulley center section

Fig 5. Welding the Mast Pulley

We are now moving towards further processing, which is fundamental to the very essence of this work: the assembly and disassembly at the scale of the generator. As shown in Fig. 6, this step is crucial to allow controlled movement of our system, composed of the wind turbine, pulley, and belt. By performing this operation on an appropriate scale, we ensure precise and efficient manipulation of our experimental setup, thus ensuring optimal conditions for conducting tests and collecting reliable data. We are reaching a critical point in our project where the incorporation of a coupling becomes indispensable. As previously mentioned, this coupling element must be rigid, and we have chosen a specific key way coupler. As shown in Fig. 7, this decision proves essential to establish a strong and stable connection between the generator and the other system components, ensuring efficient transmission of driving force.

Fig 6. Generator pulley extraction

Fig 7. Installation of the pulley on the generator

In continuation of our project, as shown in Fig. 8, we undertook the drilling of two flat iron pieces about 1-meter long. This operation aimed to create hollow rectangles, thus allowing to hold the generator while serving as a slide for its adjustment parallel to that of the wind turbine pulley

We now enter a new phase that encompasses welding the flat irons using the jig and mounting the generator with the bracket. These crucial steps aim to ensure a solid and precise fixation of the system components. By using the jig, we ensure optimal alignment of the flat irons before proceeding with welding, thus ensuring the solidity of the structure. Once these operations are completed, we mount the generator on its bracket, thereby ensuring its stability and proper functioning within the entire device. Fig. 9 illustrates these stages of the process.

Fig 8. Drilling of Flat Irons and Assembly of the Jig System

We are now embarking on another essential phase concerning the drilling of the elements required to anchor our wind turbine into the ground. This operation is of paramount importance as it ensures the stability and safety of our wind turbine once installed. By drilling the anchoring elements into the ground, we ensure a solid and durable anchorage, allowing the wind turbine to effectively withstand the forces of the wind and varying environmental conditions. Precision and rigor in this step are crucial to ensure the proper functioning and longevity of our wind system. Then, we proceed to choose the belt for our system. This step is important as the belt plays a crucial role in transmitting power between the pulley of the wind turbine and that of the generator. To do this, we accurately measure the distance between the two pulleys and determine the length of belt required based on this distance. Once this measurement is taken, we select a belt of the appropriate length, capable of bearing the workload and withstanding the environmental conditions encountered during the operation of the wind turbine. To conclude our experimental section, we need to prepare our system to be connected to essential components such as a resistor, a voltmeter, and an ammeter. These elements are crucial to achieve our specific goal of providing electricity reliably and efficiently. Finally, to achieve the desired results, Fig. 10 illustrates the outcome of the complete installation

Fig 9. Welding of flat irons using the jig and Mounting of the generator with the bracket

Fig 10. Complete system setup and parameter recording

4. PRESENTATION OF EXPERIMENTS

The experiments conducted throughout this study aim to understand the parameters defining the flow of a fluid, specifically atmospheric air, through a wind tunnel test section in the presence of a wind turbine. By measuring velocity and tension, various coefficients characterizing the behavior of the studied wind turbine were calculated. Thus, this work is divided into two parts: one focusing on the construction of the wind turbine, while the other concentrates on analyzing the impact of load on tension (voltage).

4.1 Experimental Conditions

Table 1. Conditions of the experiment

Velocity [m/s]	Pression [bar]	Temperature [C°]
13.18761		
16.68115	1.0012	25
20.43016		

Table 2. Analysis Resistance (R) and Current (I)

load	**R_1**	**R_2**	**R_3**	**R_4**	**R**
	800	440	220	220	210
1/R	0.00114	0.00227	0.00455	0.00455	0.00909
I[A]	0.25	0.5	1	1	2

Table.3 Load Assembly Procedure

	Load assembly	**R_{equi}**	**V_{dc} [v]**
load 0	R_0	0	30
load 1	R_1	880	30
load 2	R_1/R_2	293.3	29.40
load 3	$R_1/R_2/R_3$	125.7	28.20
load 4	$R_1/R_2/R_3/R_4$	80	27
load 5	$R_1/R_2/R_3/R_4/R_5$	46.31578947	25.5

4.2 Application of the Bernoulli equation for velocity calculation.

Using Bernoulli's equation (Chebel et al. 2020) between two points A and B along the streamline following the Pitot tube, we can calculate the flow velocity. This fundamental law of fluid mechanics allows us to establish a relationship between dynamic pressure, static pressure, and the density of the moving fluid. Thus, by applying this equation in the context of our experiment, we are able to determine the flow velocity inside the wind tunnel. The established equation is as follows:

$$P_A + \frac{1}{2}\rho V_A^2 = P_B + \frac{1}{2}\rho V_B^2 \tag{1}$$

where P_A and P_B represent the static pressures at points A and B respectively, V_A and V_B are the velocities at points A and B, and ρ is the fluid density. Simplifying this equation to express the velocity V, we obtain:

$$V = \sqrt{\frac{2(PA - PB)}{\rho}} \tag{2}$$

where P_A and P_B are the static pressures at points A and B respectively, and ρ is the fluid density. Therefore, the calculated velocity amounts to 12.977 m/s (for a height of 10 mm, at a temperature of 25°C).

4.3 Graphical Analysis of Experimental Data

Fig. 11 depicts the tension variation with wind tunnel velocity. It's clear that tension is proportional to the applied velocity. As the wind tunnel velocity increases, the measured tension also increases. This linear relationship between tension and wind tunnel velocity is consistent with the basic principles of fluid dynamics, where an increase in flow velocity leads to an increase in dynamic pressure, resulting in an increase in measured tension.

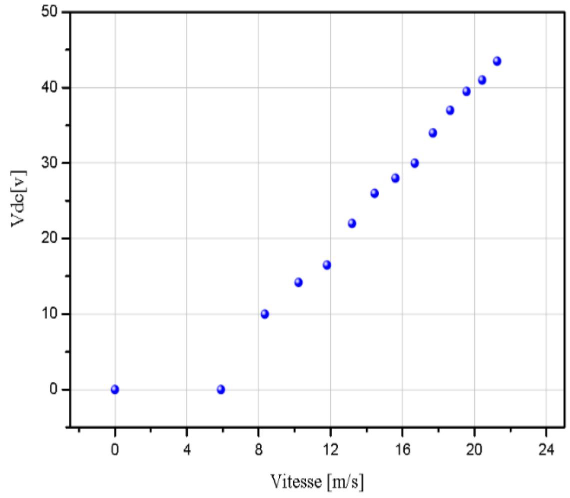

Fig 11. Distribution of voltage as a function of velocity

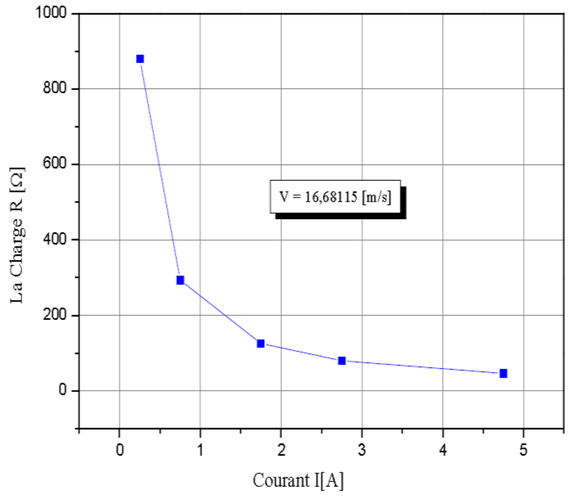

Fig 12. Current distribution as a function of the load

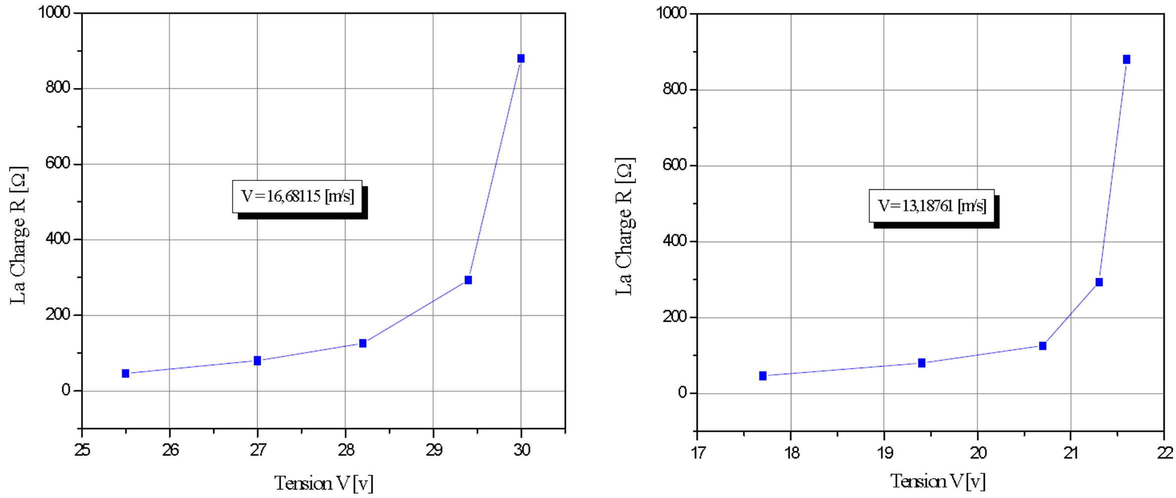

Fig. 13&14. Voltage distribution as a function of velocity

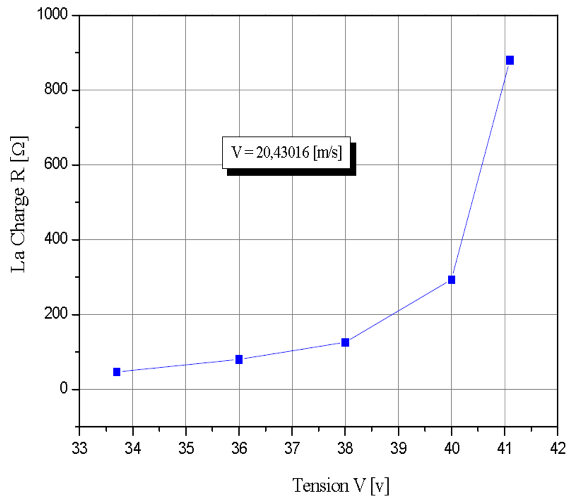

Fig 15. Voltage distribution as a function of velocity

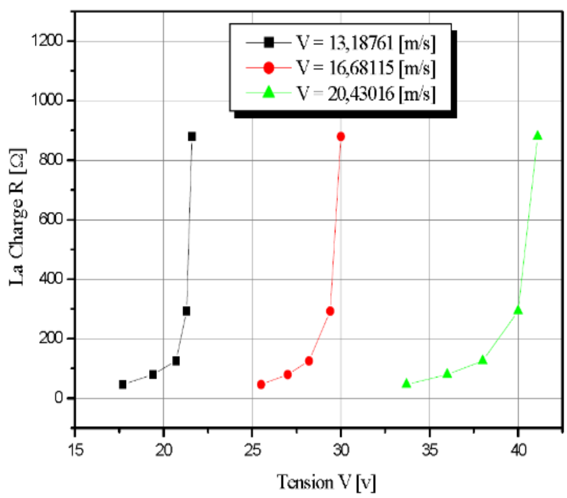

Fig 16. Voltage distribution as a function of multiple velocities

4.4 Interpretation of the graphs

Fig. 12, Fig. 13, Fig. 14, and Fig.15 reveal the variations in current and voltage with respect to the load. During load testing, various resistance loads are applied to the generator terminals to simulate different load conditions. The results indicate a decrease in the load current as the load increases, following an inverse relationship. Simultaneously, the load voltage increases with the applied load, highlighting a proportional relationship between voltage and load. These findings underscore the consistent response of the electrical system to load fluctuations, crucial for understanding and optimizing generator performance under different conditions. This relationship is described by Ohm's law (Tran et al. 2010), which states that resistance (R) equals voltage (V) divided by current (I), or:

$$R = \frac{V}{I} \tag{3}$$

The power law, which we used to calculate the power produced by our system, is expressed by the following formula:

$$Po = V \times I \tag{4}$$

where:

- Po is the power in watts (W).
- V is the voltage in volts (V).
- I is the current in amperes (A).

This law connects electrical power to voltage and current in a circuit (Al Noman et al. 2022).

The data presented in Fig.16 provide insight into how voltage varies with load and speed. It is noteworthy that the charging voltage follows a proportional relationship with speed. Specifically, as the wind tunnel speed increases, the recorded charging voltage also increases proportionally. This observation highlights an important characteristic of the system where wind tunnel speed directly influences the generated voltage. An increase in wind tunnel speed leads to a corresponding increase in charging voltage, suggesting a linear relationship between these two variables. This relationship between voltage and speed offers valuable insights for understanding and optimizing system performance under varying wind tunnel speed conditions.

5. CONCLUSION

This experimental study of the vertical axis Savonius wind turbine has shed light on several essential aspects of its operation and performance. Among the key points highlighted in this research:

- A linear relationship between the charging voltage and the wind speed, emphasizing the direct impact of wind speed on electricity production.
- An inversely proportional relationship between the charging current and the applied load, confirming the predictability of the system (Rochman et al. 2022).
- The crucial importance of precision in measurements and calculations to obtain reliable and actionable data.
- Valuable insights for the design and optimization of vertical axis wind turbines.

- The importance of understanding the complex interactions between the variables involved in wind energy production.

APPENDIX

Table 4. Table of Calculated Power in the System

		Lamp
I [A]	**Po [watt]**	18
0	0	0
0.25	7.5	0
0.75	22.05	1
1.75	49.35	3
2.75	74.25	4
4.75	121.13	7

NOMENCLATURE

v	Velocity [m/s]	I	Current [A]
P	Pression [bar]	V_{dc}	Voltage Direct Current [v]
T	Temperature [°C]	ρ	the fluid density [kg/m^3]
R	Load (resistance)	Po	Power [W]

ABBREVIATIONS

VAWT: Vertical Axis Wind Turbine
HAWT: Horizontal Axis Wind Turbine

REFERENCES

Al Noman, A., Tasneem, Z., Sahed, Md. F., Muyeen, S.M., Kumar Das, S., Alam, F. (2022). Towards next generation Savonius wind turbine: Artificial intelligence in blade design trends and framework. Renewable and Sustainable Energy Reviews, 168, 112531. doi: 10.1016/j.rser.2022.112531.

Alexander, A.J. Holownia, B.P. (1978). Wind tunnel tests on a Savonius rotor. Journal of Wind Engineering and Industrial Aerodynamics, 3(4), 343‑351. doi: 10.1016/0167-6105(78)90037-5

Chebel, A., Benretem, A., Dobrev, I., Barkati, B. (2020). Comparative study of two control strategies proportional integral and fuzzy logic for the control of a doubly fed induction generator dedicated to a wind application. International Journal of Power Electronics and Drive Systems,11, 263-274. doi: 10.11591/ijpeds.v11.i1.pp263-274

Mojola, O.O. (1985). On the aerodynamic design of the savonius windmill rotor. Journal of Wind Engineering and Industrial Aerodynamics, 21(2), 223‑231. doi: 10.1016/0167-6105(85)90005-4

Ricci, R., Romagnoli, R., Montelpare, S., Vitali, D. (2016). Experimental study on a Savonius wind rotor for street lighting systems. Applied Energy, 161, 143‑152. doi : 10.1016/j.apenergy.2015.10.012

Rochman, S., Wijayakusuma, K., Rolos, R. J. J. (2022). Design and construction of vertical helix savonius wind turbine for public street lighting. Best : Journal of Applied Electrical, Science, & Technology, 4(2). https:// doi.org/10.36456/best.vol4.no2.6158

Saha, U. K., Thotla, S. and Maity, D. (2008). Optimum design configuration of Savonius rotor through wind tunnel experiments. Journal of Wind Engineering and Industrial Aerodynamics, 96(8), 1359‑1375.

Tran, D.H., Sareni, B., Roboam, X., Espanet, C. (2010). Integrated Optimal Design of a Passive Wind Turbine System: An Experimental Validation. IEEE Transactions on Sustainable Energy, 1. doi: 10.1109/TSTE.2010.2046685